Paper No. T3-1.4, pp. 1-6

15th INTERNATIONAL SYMPOSIUM on POWER ELECTRONICS - Ee 2009
XV Međunarodni simpozijum Energetska elektronika – Ee 2009
NOVI SAD, REPUBLIC OF SERBIA, October 28th - 30th, 2009

OPTIMUM TORQUE/CURRENT CONTROL OF DUAL-PMSM SINGLE-VSI DRIVE

A. Del Pizzo, D. Iannuzzi, I. Spina
Dept. of Electrical Engineering, University of Naples "Federico II" - Italy

Abstract: *The paper deals with isotropic PM-brushless drives in configuration "single-inverter, dual-motor" operating with un-balanced load-torques. An innovative control algorithm is pre-sented. It is suitable to minimize the resultant armature current needed to obtain an assigned resultant motor torque, whatever is the load unbalance. Simplified analytical expressions are given in order to quickly evaluate optimized reference cur-rents with good approximation. From these reference values, a predictive feeding algorithm evaluates the reference voltage space-vector for the inverter supplying the two motors in parallel. Current and torque oscillation, torque/current ratio, dynamic response and stability are the mainly observed quantities. Effectiveness of proposed control techniques are highlighted.*

Key Words: ***PMSM motor/Dual Motor/Optimized Control***

1. INTRODUCTION

Vector and predictive control of ac drives are widely investigated and used in many application fields with reference to the classical configuration "single-inverter, single-motor". A considerable interest has been also devoted to the control of drives composed by a single inverter feeding more motors in parallel. Main targets of these drives are reduced sizes and costs with respect to the single motor drives, either in industrial or in traction applications. Some scientific papers and practical applications can be found concerning single-inverter dual-motor drives which use induction motors, either with scalar or vector control [1, 2]. In these cases, for control purposes the parallel connected motors are assumed equivalent to one single motor. The majority of the papers refers to a dynamic machine model of the combined, parallel connected, dual induction motor system [3]. In addition, these papers illustrate torque-control methods based on the previous model, which enable mean and differential torque to be controlled during transient and steady-state operations.

The above described problems are not widely dealt with in the literature in case of PM-brushless motors supplied in parallel by a single inverter, as it can occur in those traction or industrial applications where PM motors are more and more requested.

In these multi-motor drives either steady-state or transient operations could be more critical than in case of induction motors. This is due to the constancy of the rotor flux and to the absence of a rotor winding able to positively react in case of transient operations. In fact, considering two motors supplied in parallel by same frequency and voltage and with load unbalance, while in case of induction motors the rotor speeds get different values depending on the load-torque, in case of PM-brushless synchronous motors the rotor speeds are equal at steady-state, whatever is the unbalance values. As a consequence, when the load-torque of one motor suddenly varies, a risk of instability could occur if the angle between the armature voltage and e.m.f. vectors runs over $\pi/2$.

In the technical literature some authors have proposed a steady-state control of torque angle of only a motor a time, selecting that one with highest load-torque [4, 6, 7].

Other authors have suggested simple control configurations based on two main criteria: in a first case the two real motors are substituted by a single "equivalent" motor, by suitably handling measured current and speed values of each motor; in a second case the control and feeding algorithms are separately applied for the two motors and the resultant converter voltage is obtained by properly manipulating two voltage space-vectors separately evaluated. In this paper a new control technique is presented: on the basis of the measured speed and of the reference torque of both motors, the reference currents are evaluated in analytical way, imposing an optimizing condition to reduce the inverter size. A predictive feeding algorithm is used to evaluate the reference voltage space-vector for the inverter supplying the two motors in parallel.

2. MATHEMATICAL MODEL

We refer to two isotropic PM-brushless motors supplied in parallel by a single inverter (fig.1).

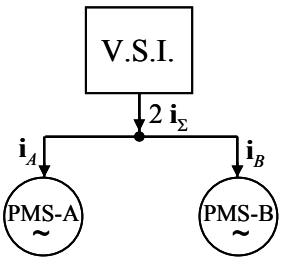

Fig.1- Schematic representation of a single-inverter dual-motor configuration

We assume that parameters and rated values of motors "A" and "B" are equal, but each of them can be arbitrarily charged (unbalanced loads). Assuming sinusoidal the induced e.m.f. for both motors, their mathematical models in the respective rotor reference systems (superscript *a* or *b*) are expressed by:

$$\begin{cases} \mathbf{v}_A^a = R\cdot\mathbf{i}_A^a + L_s\dfrac{d}{dt}\mathbf{i}_A^a + jp\,\omega_{r,A}L_s\mathbf{i}_A^a + jp\,\omega_{r,A}\,\Phi_{r,A} \\ T_A - T_{L,A} = J_A\dfrac{d}{dt}\omega_{r,A};\;\; T_A = \dfrac{3}{2}p\,\Phi_{r,A}\Im m\left\{\mathbf{i}_A^a\right\} \\ \omega_{r,A} = \dfrac{d}{dt}\vartheta_A \end{cases} \qquad (1)$$

$$\begin{cases} \mathbf{v}_B^b = R\cdot\mathbf{i}_B^b + L_s\dfrac{d}{dt}\mathbf{i}_B^b + jp\,\omega_{r,B}L_s\mathbf{i}_B^b + jp\,\omega_{r,B}\,\Phi_{r,B} \\ T_B - T_{L,B} = J_B\dfrac{d}{dt}\omega_{r,B};\;\; T_B = \dfrac{3}{2}p\,\Phi_{r,B}\Im m\left\{\mathbf{i}_B^b\right\} \\ \omega_{r,B} = \dfrac{d}{dt}\vartheta_B \end{cases}$$

where $\mathbf{i}_A$, $\mathbf{i}_B$ are the current space-vectors of motors "A", "B", and the other symbols are explained in the list at the end of the paper. Denoting by 2ψ the angular displacement between the axes of the rotor fluxes $\mathbf{\Phi}_A$ and $\mathbf{\Phi}_B$ (fig.2), the equivalent *d*-axis is assumed in the mean position between $\mathbf{\Phi}_A$ and $\mathbf{\Phi}_B$, while the flux magnitude produced by permanent magnets is the same ($\Phi_{r,A} = \Phi_{r,B} = \Phi_r$), since we suppose the two motors equal.

In the new equivalent reference system (mean flux position), eq.s (1) become:

$$\begin{cases} \mathbf{v}_\Sigma = R\cdot\mathbf{i}_\Sigma + L_s\dfrac{d}{dt}\mathbf{i}_\Sigma + jp\,\omega_{r\Sigma}L_s\mathbf{i}_\Sigma + jp\,\omega_{r\Delta}L_s\mathbf{i}_\Delta + \\ \quad + jp\,\omega_{r\Sigma}\,\Phi_r\cos\psi + p\,\omega_{r\Delta}\,\Phi_r\sin\psi \\ T_\Sigma - T_{L,\Sigma} = J\dfrac{d}{dt}\omega_{r\Sigma} \quad \text{with: } T_\Sigma = \dfrac{3}{2}p\,\Phi_r\left(i_{\Sigma q}\cos\psi + i_{\Delta d}\sin\psi\right) \\ \\ 0 = R\cdot\mathbf{i}_\Delta + L_s\dfrac{d}{dt}\mathbf{i}_\Delta + jp\,\omega_{r\Sigma}L_s\mathbf{i}_\Delta + jp\,\omega_{r\Delta}L_s\mathbf{i}_\Sigma + \\ \quad + p\,\omega_{r\Sigma}\,\Phi_r\sin\psi + jp\,\omega_{r\Delta}\,\Phi_r\cos\psi \\ T_\Delta - T_{L,\Delta} = J\dfrac{d}{dt}\omega_{r\Delta} \quad \text{with: } T_\Delta = \dfrac{3}{2}p\,\Phi_r\left(i_{\Delta q}\cos\psi + i_{\Sigma d}\sin\psi\right) \end{cases}$$

where subscripts "Σ" and "Δ" refer respectively to "mean" and "differential" quantities, defined as (for a generic variable *G*):

$$G_\Sigma = \frac{G_A + G_B}{2} \quad ; \quad G_\Delta = \frac{G_A - G_B}{2}.$$

In steady-state operations, denoting by $\omega_r = \omega_{r,A} = \omega_{r,B}$ the rotor speed of both motors, the mathematical model is given by:

$$\begin{cases} \mathbf{V}_\Sigma = R\cdot\mathbf{I}_\Sigma + jp\,\omega_r L_s\mathbf{I}_\Sigma + jp\,\omega_r\,\Phi_r\cos\psi \\ 0 \;\; = R\cdot\mathbf{I}_\Delta + jp\,\omega_r L_s\mathbf{I}_\Delta + p\,\omega_r\,\Phi_r\sin\psi \\ T_\Sigma = \dfrac{3}{2}p\,\Phi_r\left(I_{\Sigma q}\cos\psi + I_{\Delta d}\sin\psi\right) \\ T_\Delta = \dfrac{3}{2}p\,\Phi_r\left(I_{\Delta q}\cos\psi + I_{\Sigma d}\sin\psi\right) \end{cases} \qquad (2)$$

In a control problem, ω_r, T_Σ and T_Δ are known quantities; then, the system (2) corresponds to a set of six real equations with seven real unknown quantities ($\mathbf{V}_\Sigma, \mathbf{I}_\Sigma, \mathbf{I}_\Delta, \psi$). Due to this degree of freedom, one 'auxiliary condition' is needed in order to solve the system (2). This condition could represent the *control algorithm* for the considered dual drive.

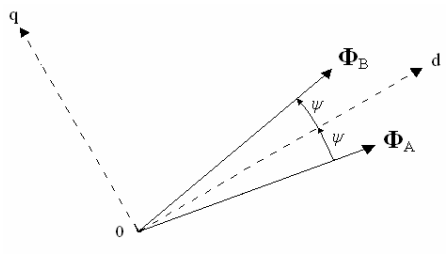

Fig. 2 -Reference system

3. CURRENT CONTROL ALGORITHM

A noticeable quantity is the torque to current ratio:

$$\rho = \frac{T_A + T_B}{\left|\mathbf{I}_A + \mathbf{I}_B\right|} = \frac{T_\Sigma}{\left|\mathbf{I}_\Sigma\right|} = \frac{T_\Sigma}{I_\Sigma} \qquad (3)$$

On the basis of (2) ρ can be expressed as:

$$\rho = \frac{A\sin\psi\cos\psi}{\sqrt{\left(B\cos\psi + C\sin\psi\cos^2\psi\right)^2 + \left(D\sin\psi + E\sin^3\psi\right)^2}}$$

$$\rightarrow \rho = \rho\left(T_A, \frac{T_B}{T_A}, \omega_r, \psi\right)$$

where:

$$A = T_\Sigma 3p\,\Phi_r Z^2; \quad B = 2T_\Delta Z^2; \qquad C = -3p^3\omega_r{}^2\Phi_r{}^2 L$$

$$D = 2T_\Sigma Z^2 \quad ; \quad E = 3p^2\omega_r\Phi_r{}^2 R; \quad Z = \sqrt{R^2 + \left(p\omega_r L\right)^2}$$

The qualitative curve $\rho(\psi)$ is plotted in fig.3*a* for assigned values of ω_r, T_A and of load-unbalance $r = T_B/T_A$. This behaviour suggests to state as control algorithm the condition:

$$\max\left\{\frac{T_\Sigma}{I_\Sigma}\right\} \Rightarrow \frac{\partial}{\partial\psi}\left(\frac{T_\Sigma}{I_\Sigma}\right)=\frac{\partial\rho}{\partial\psi}=0 \qquad (4)$$

which is also suitable to minimize the size of the feeding inverter.

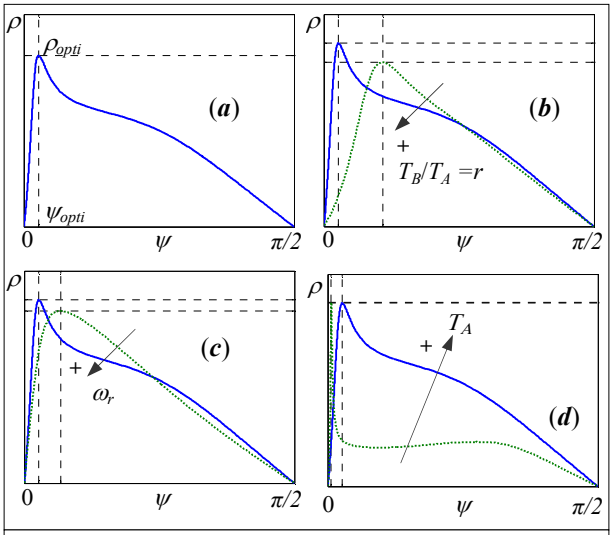

Fig.3 - Behaviour of ρ as a function of ψ (diagram ***a***) and for different values of r, ω_r, T_A (diagrams ***b***, ***c***, ***d***)

In case of balanced shaft loads, eq.(4) corresponds to separate maximization of both torque/current ratios $\{T_A/|\mathbf{I}_A|\}$ and $\{T_B/|\mathbf{I}_B|\}$ for the two motors.

From (2) it is easy to verify that the d-q components of the "mean" current $\mathbf{I}_\Sigma = I_{\Sigma d} + j\, I_{\Sigma q}$ are :

$$\begin{cases} I_{\Sigma d} = \dfrac{2T_\Delta}{3p\Phi_r}\dfrac{1}{\sin\psi} - \dfrac{(p\omega_r)^2\Phi_r L}{R^2+(p\omega_r L)^2}\cos\psi \\ I_{\Sigma q} = \dfrac{2T_\Sigma}{3p\Phi_r}\dfrac{1}{\cos\psi} + \dfrac{p\omega_r\Phi_r R}{R^2+(p\omega_r L)^2}\dfrac{\sin^2\psi}{\cos\psi} \end{cases} \qquad (5)$$

By substituting (5) in (4) we deduce that the derivative (4) becomes a transcendent function of ψ, not solvable in analytical way. However, we can demonstrate that the function $\rho = T_\Sigma/I_\Sigma$ is positive in the interval $\psi \in (0, \pi/2)$ and $\rho=0$ either for $\psi=0$ or $\psi=\pi/2$. Consequently, ρ has a maximum ρ_{optim} in the interval $(0, \pi/2)$ in correspondence of a ψ_{optim} value (see fig.3*a*) . Diagrams *b*, *c* and *d* of fig.3 show the shifting of the point (ψ_{optim}, ρ_{optim}) in correspondence of different values of either $r = T_B/T_A$, or ω_r or T_A respectively.

With reference to a pair of equal motors, whose rated parameters are in tab.I (see section VI), figs.4 show the behaviour ρ_{optim} against r (i.e. for different unbalanced conditions) in correspondence of different load torques T_A and for two different steady-state rotor speeds ω_r (continuous lines).

In correspondence of relatively low values of load unbalance, the angle ψ_{optim} is enough small to assume:

$$\sin\psi \cong \psi \quad ; \quad \cos\psi \cong 1 \qquad (6)$$

Introducing this approximation, eq.(4) becomes a 1st degree equation in ψ and a very simple analytical expression of ψ_{optim} can be found:

$$\psi_{optim}^{(a)} = \frac{2T_\Delta\left[R^2+(p\omega_r L)^2\right]}{3p^3\omega_r{}^2\Phi_r{}^2 L} \text{ ; with } T_\Delta = T_A\frac{1-r}{2} \qquad (7)$$

where $\psi_{optim}^{(a)}$ is the approximated value of ψ which maximizes the $\rho = T_\Sigma/I_\Sigma$ ratio. It is independent on T_Σ and can be analytically determined. The correspondent curves of approximated ρ_{optim} are plotted against r in fig.4 with dotted lines. As we can see, they are generally very close to the not simplified curves and differ from them only for low values of r (≡ high load unbalance).

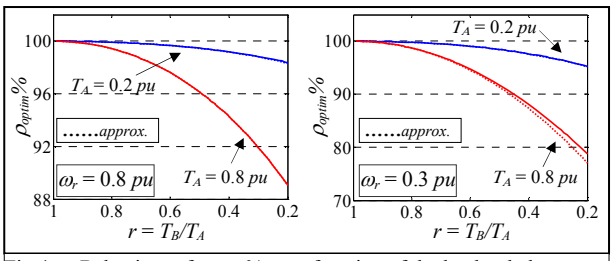

Fig.4 – Behaviour of ρ_{optim} % as a function of the load-unbalance r, for two different speed values and for low and high load-

The validity of the approximation (6) is also confirmed by the compared behaviours of ψ_{optim} and $\psi_{optim}^{(a)}$ in fig.5 which refers to the same cases analysed in fig.4.

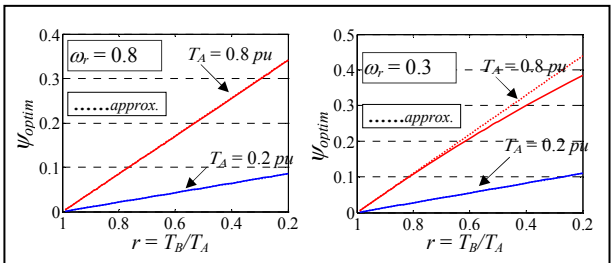

Fig.5 – Behaviour of ψ_{optim} and $\psi_{optim}^{(a)}$ as a function of the load-unbalance r, for two different speed and load-torque values.

From fig.s 4, 5 we also deduce that as higher load unbalance is, as lower the maximum value of ρ_{optim} and higher the shift angle ψ_{optim} .

In correspondence of the optimized condition (3), in fig.6 magnitude I_Σ of the mean current is drawn against unbalance r, for different speed and load conditions.

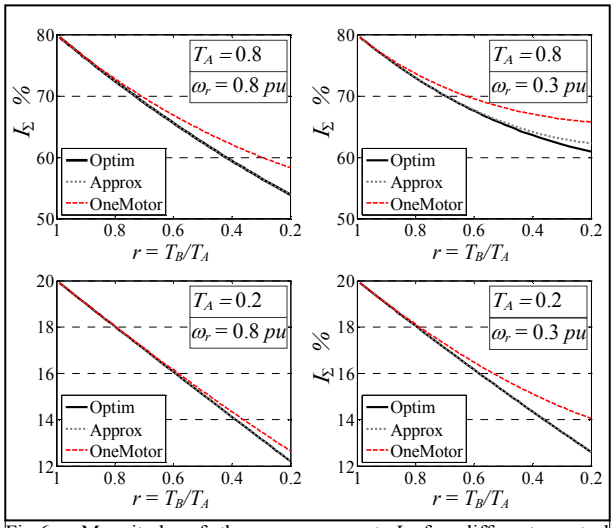

Fig.6 – Magnitude of the mean current I_Σ for different control techniques in some speed and torque operating condition

These values are compared to the approximated ones, obtained using eq.s (5)-(7), and to the ones obtained using a different control technique, named "one motor control", better explained in section V [4]. While the differences between exact and approximated I_Σ curves are very small, the current I_Σ assumes considerably higher values in the case of the "one motor control" technique, with negative consequences on the converter size.

4. PREDICTIVE FEEDING ALGORITHM

A predictive feeding algorithm can be useful to reduce current and torque distortion with respect to the use of hysteresis or PI current controllers [5].

We consider the discrete stator model of isotropic PM motors with all the electric quantities expressed in the mean *d,q* reference frame:

$$L_s \frac{d}{dt}\mathbf{i} + \dot{Z}_s\ \mathbf{i}\ =\ \mathbf{v}_n - \boldsymbol{\varepsilon}_n\,; \qquad \text{for } t\in(t_n,\, t_{n+1}) \qquad (8)$$

where: $\dot{Z}_s = R + j\,p\,\omega_r\,L_s \quad ; \quad \boldsymbol{\varepsilon}_n = j\,p\,\omega_{r,n}\Phi_r \cos\psi_n$

In (8) $\mathbf{v}_n$ and $\mathbf{e}_n$ are evaluated at a generic sampling instant t_n. During the interval $(t_n,\ t_{n+1})$, thanks to some suitable assumptions in the model (8), we can evaluate the reference voltage $\mathbf{v}^*_{n+1} = v^*_{d,n+1} + j\,v^*_{q,n+1}$ to be applied at the instant t_{n+1}, in order to obtain –at the instant t_{n+2}– armature current $\mathbf{i}_{n+2}$ equal to the reference current at t_n (i.e, $\mathbf{i}_{n+2} = \mathbf{i}^*_n$). We have:

$$\mathbf{v}^*_{n+1} = \boldsymbol{\varepsilon}_n + \dot{Z}_s \frac{\mathbf{i}^*_{\Sigma,n} - \dot{\alpha}_t\left[\dot{\alpha}_t\left(\mathbf{i}_{\Sigma,n} - \dfrac{\mathbf{v}_n - \varepsilon_n}{\dot{Z}_s}\right) + \dfrac{\mathbf{v}_n - \boldsymbol{\varepsilon}_n}{\dot{Z}_s}\right]}{1 - \dot{\alpha}_t} \qquad (9)$$

where: $\dot{\alpha}_t = \mathrm{e}^{\frac{\dot{Z}_s}{L_s}\Delta t}$ with: $\Delta t = t_{n+1} - t_n$.

The feeding algorithm (9) needs only the knowledge of the reference current $\mathbf{i}^*_{\Sigma,n} = i^*_{\Sigma d,n} + j\ i^*_{\Sigma q,n}$ and of the motor state in t_n [i.e.: $\psi_n, i_{\Sigma d,n}, i_{\Sigma q,n}, \omega_{r,n} = (\omega_{r,A,n} + \omega_{r,B,n})/2$].

5. CONTROL DIAGRAM

The used speed control circuit is described in fig.7.

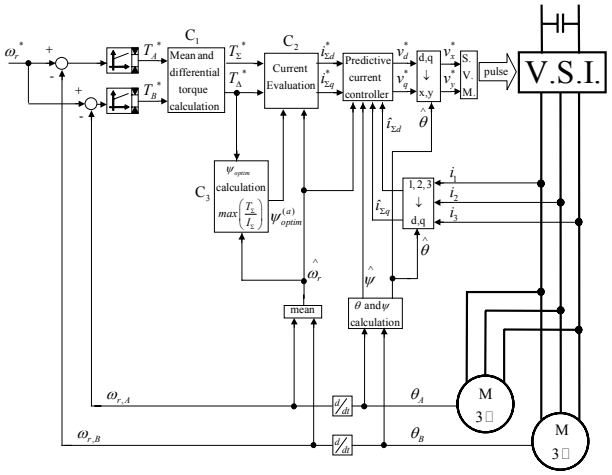

Fig. 7 – "Proposed Control" Circuit

The actual speed of each motor is separately detected and compared with the imposed ω^*_r speed value. From the two reference torques T^*_A and T^*_B, the block C_1 evaluates the mean and differential reference torques T^*_Σ, T^*_Δ and, in cascade, C_2 evaluates the reference currents $i^*_{\Sigma d}, i^*_{\Sigma q}$ by means of eq.(5) and using $\psi^{(a)}_{optim}$ calculated by block C_3 corresponding to eq.(7). An encoder on each rotor shaft separately detects actual values of position and speed. The estimated *d,q* components $\hat{i}_{\Sigma d}$, $\hat{i}_{\Sigma q}$ of the actual mean currents are derived from measurement of the resultant inverter currents.

Reference and actual currents, together with mean actual speed $\hat{\omega}_r$, are used by the "predictive current controller" to evaluate the reference voltages v^*_d, v^*_q, which are transformed in stator coordinates *x,y* using the mean angular position $\hat{\theta} = (\theta_A + \theta_B)/2$. Comparing the proposed control technique with the ones in literature [6] we can observe that in fig.7 the reference currents $\hat{i}_{\Sigma d}$, $\hat{i}_{\Sigma q}$ are evaluated by imposing an optimizing analytical criterion while in [6] they are obtained simply adding the values separately obtained for the two motors. Another advantage of the proposed control is that only the feedback of the resultant stator currents is used (instead of a double current loop).

In next section the numerical results of the "proposed control technique" are compared to the one obtained using the simpler control diagram of fig.8 ("one-motor control"), as proposed in the literature [4].

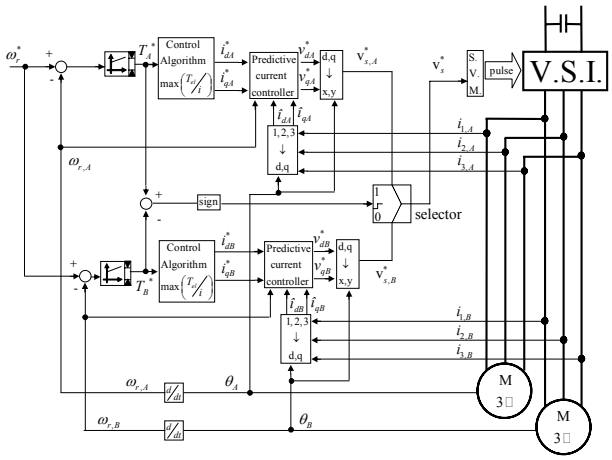

Fig. 8 – "One-Motor Control" Circuit

6. NUMERICAL ANALISYS

A numerical analysis is carried out with reference to two three-phase PM brushless motors having equal rated values, as summarized in tabI.

Table 1. *Main Data of both PM motors*

Rated power P_R	74 *kW*	Rated speed $\omega_{r,R}$	33.5 *rad s*$^{-1}$
Pole-pair p	8	Rotor inertia J_r	0.9 *kgm*^{2}
Rated voltage V_R	570 *V*	Armature inductance L	5.7 *mH*
Rated current I_R	128 *A*	Armature resistance R	0.27 Ω

The average switching frequency of the IGBT-SVM voltage source inverter is about 2 *kHz*. The load torque characteristic of both motors is assumed linear in function of the angular speed. Reference speed is set to $\omega_r^* = 0.8\,\omega_{r,R}$ for the case in fig.9.

Actual speeds, torques and currents of both motors A and B are plotted in fig.9, together with the mean currents $i_{\Sigma d}$, $i_{\Sigma q}$, the voltage amplitude and the shifting angle between the two rotor polar axes.

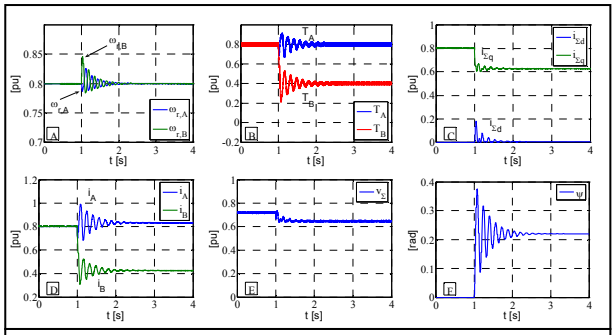

Fig.9 - Numerical results of "proposed control" technique for ω_r^*= 0.8 pu

The letters inside the figure have the following meaning: *A*) actual speeds of both motors; *B*) electromagnetic and load torque of both motors; *C*) *d*-axis and *q*-axis components of the mean current; *D*) current magnitude of both motors; *E*) magnitude of reference voltage space-vector; *F*) electrical angle ψ between the two rotor frames.

The load conditions are equal for both motors until the instant t=1 *s* and correspond to load-torque values $T_{A,L}$=$T_{B,L}$=0.8 pu of the rated torque. At the instant t=1 *s* a step variation from 0.8 to 0.4 pu (50%) of the load torque is introduced for motor B, in order to test the capability of the system to get a steady-state condition together with acceptable values of amplitude both of torque and current oscillations. From the diagrams we can deduce that the decrease of the load torque $T_{B,L}$ produces transient variations in all the electromechanical quantities of both motors A and B.

Referring to fig.9, when steady-state is reached, the speeds of the two motors assume again the initial value 0.8 $\omega_{r,R}$; the electromagnetic torques of both motors follow the respective load values; the *d*-component $i_{\Sigma d}$ of the mean current is practically equal to zero, while the *q*-component $i_{\Sigma q}$ decreases of about 25%. The angular positions of the two rotors assume different values and the shift-angle between them remains constant.

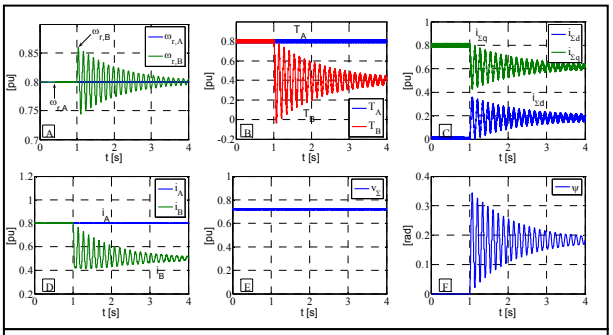

Fig.10 – Numerical results of "one-motor control" technique for ω_r^*= 0.8 pu

The diagrams of fig.10 represent the same quantities of fig.9, in equal operating conditions, but with reference to the control circuit of fig.8 ("one-motor control").

The following fig.s 11,12 show analogous quantities of fig.s 9,10 with reference to low speed operating condition.

Comparing the results of fig.s 9,11 to the ones of fig.10, 12, it is easy to deduce that the "proposed control technique" (circuit in fig.7) gives rise to better performance both in steady-state and dynamic operations, with respect to the "one-motor control" circuit in fig.8. In fact, $i_{\Sigma d}$ in fig.10c&12c assumes stady-state values considerably higher than in the correspondent ones in fig.9c&11c. Moreover, it is evident the greater time needed by the "one-motor control" together with a greater magnitude of torque, speed and current oscillations.

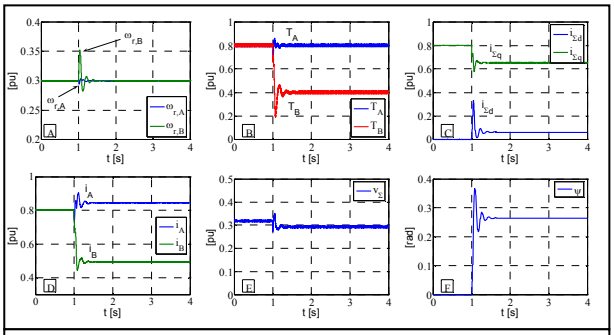

Fig.11 - Numerical results of "proposed control" technique for ω_r^*= 0.3 pu

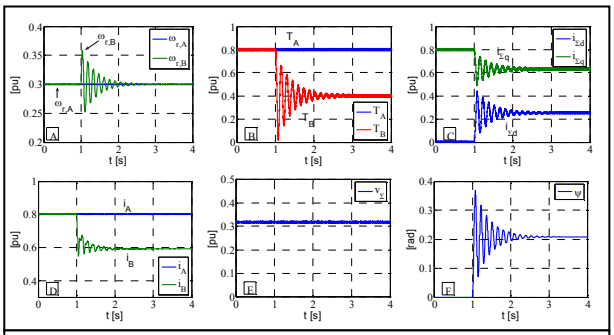

Fig.12 - Numerical results of "one-motor control" technique for ω_r^*= 0.3 pu

7. SHORT CONLUSIVE REMARKS

With reference to a drive composed by a single inverter feeding two isotropic PM brushless motors in parallel, a new control technique is proposed in order to manage load unbalances. It is based on a control algorithm and a feeding algorithm in cascade. The feeding algorithm uses the predictive voltage evaluation already presented in [6], that is able to obtain low values of current distortion and torque pulsation. The control algorithm is based on an auxiliary condition which optimizes the set of two motors, aiming to maximize the ratio (resultant torque)/(resultant current).

The main features of the proposed control are: a reduced number of current transducers, steady-state operations with the minimum input current for every resultant load-torque in case of load unbalance (reduction of inverter size), reduced over-shoot and acceptable dynamics in transient operations, good stability also in presence of heavy variations of the load torque on only one motor.

SHORT LIST OF SYMBOLS

$\mathbf{I}_A, \mathbf{I}_B$	steady-state current of motor A, B
$\mathbf{I}_\Sigma, \mathbf{I}_\Delta$	steady-state mean and differential current
L	armature inductance
p	pole-pair
R	armature phase resistance
$T_{A,L}, T_{B,L}$	load torque of motor A, B
$\theta_A; \theta_B$	angular position of rotor A, B
Φ_r	air-gap flux of rotor magnets
ω_r	rotor angular speed
$\omega_{r,R}$	rated value of rotor angular speed
ψ_{optim}	optimized shift angle between rotor polar axes

8. REFERENCES

[1] Y. Matsumoto, C. Osawa, T. Mizukami, S. Ozaki: "*A Stator-Flux Based Vector Control Method for Parallel-Connected Multiple Induction Motors Fed by a Single Inverter*". Proc. IEEE APEC'98, pp. 575-580, 1998.

[2] I. Ando, M. Sato, M. Sazawa, K. Ohishi: "*High efficient speed control of parallel-connected induction motors with unbalanced load condition using one inverter*", Proc. IEEE-IECON'04, pp. 1361 - 1366, vol. 2, 2004.

[3] Wang Ruxi, Wang Yue, Dong Qiang, He Yanhui, Wang Zhaoan: "*Study of Control Methodology for Single Inverter Parallel Connected Dual Induction Motors Based on the Dynamic Model*". Proc. IEEE-PESC Conference, pp.1-7, 2006.

[4] D. Bidart, M. Pietrzak-David, P. Maussion; M. Fadel: "*Mono inverter dual parallel PMSM - structure and control strategy*". IECON 2008. 34th Annual Conference of IEEE 10-13 Nov. 2008 Page(s):268 – 273

[5] J. Maciejowski, "*Predictive Control*". Englewood Cliffs, NJ: Prentice- Hall, 2002.

[6] M. S. D. Acampa, A. Del Pizzo, D. Iannuzzi, I. Spina : "*Predictive control technique of single inverter dual motor AC-brushless drives*". Proceedings of the XVIII International Conference on Electrical Machines ICEM 2008, Sept. 6-9, 2008 Vilamoura, Algarve, Portugal.

[7] M. S. D. Acampa, A. Del Pizzo, D. Iannuzzi: "*Optimized control technique of single inverter dual motor AC-brushless drive*". 43rd International UPEC, Sept. 1-4, 2008 Padova, Italy.

[8] B. Wu, S. B. Dewan, P. C. Sen. "*A Modified Current Source Inverter (MCSI) for a multiple induction motor drive system*". Power Electronics, IEEE Transactions on, 3(1):10–16, 1988.

[9] J. Okabe, A. Kumamoto, Y. Hirane: "*Independent closed-loop control of two induction motors paralleled to a single inverter and its applications to an automatically guided carrier vehicle*", Proc. IEEE-IECON'84, pp.180-185.

[10] P. M. Kelecy, R. D. Lorenz: "Control Methodology for Single Inverter, Parallel Connected Dual Induction Motor Drives for Electric Vehicles". Proc. PESC'94, pp. 987-991, 1994.